Strain relaxation from annealing of SiGe heterostructures for qubits

Special Collection: Semiconductor Physics: Plasma, Thermal, Elastic, and Acoustic Phenomena

Yujia Liu ✉ 🆔 ; Kevin-Peter Gradwohl; Chen-Hsun Lu 🆔 ; Kaspars Dadzis; Yuji Yamamoto 🆔 ;
Lucas Becker 🆔 ; Peter Storck; Thilo Remmele; Torsten Boeck; Carsten Richter 🆔 ; Martin Albrecht 🆔

Check for updates

View Online

Export Citation

CrossMark

AIP Publishing

Strain relaxation from annealing of SiGe heterostructures for qubits

Yujia Liu,[1,a)] Kevin-Peter Gradwohl,[1] Chen-Hsun Lu,[1] Kaspars Dadzis,[1] Yuji Yamamoto,[2] Lucas Becker,[3]
Peter Storck,[3] Thilo Remmele,[1] Torsten Boeck,[1] Carsten Richter,[1] and Martin Albrecht[1]

AFFILIATIONS

[1]Leibniz-Institut für Kristallzüchtung, Max-Born-Straße 2, 12489 Berlin, Germany
[2]IHP – Leibniz-Institut für innovative Mikroelektronik, Im Technologiepark 25, 15236 Frankfurt (Oder), Germany
[3]Siltronic AG, Einsteinstraße 172, 81677 Munich, Germany

Note: This paper is part of the Special Topic on Semiconductor Physics: Plasma, Thermal, Elastic, and Acoustic Phenomena.
a)**Author to whom correspondence should be addressed:** yujia.liu@ikz-berlin.de

ABSTRACT

The misfit dislocation formation related to plastic strain relaxation in Si or Ge quantum well layers in SiGe heterostructures for spin qubits tends to negatively affect the qubit behaviors. Therefore, it is essential to understand and then suppress the misfit dislocation formation in the quantum well layers in order to achieve high-performance qubits. In this work, we studied the misfit dislocation propagation kinetics and interactions by annealing the strained Si or Ge layers grown by molecular beam epitaxy. The annealing temperatures are from 500 to 600 °C for Si layers and from 300 to 400 °C for Ge layers. The misfit dislocations were investigated by electron channeling contrast imaging. Our results show that the misfit dislocation propagation is a thermally activated process. Alongside, the blocking and unblocking interactions during misfit dislocations were also observed. The blocking interactions will reduce the strain relaxation according to theoretical calculation. These observations imply that it is possible to suppress the misfit dislocation formation kinetically by reducing the temperatures during the SiGe heterostructure epitaxy and post-epitaxy processes for developing well-functional SiGe-based spin qubits.

I. INTRODUCTION

The spin states of electrons in Si quantum well layers[1–4] or holes in Ge quantum well layers[5–7] in SiGe heterostructures are outstanding candidates for large-scale integration of fault-tolerant qubits for solid state-based quantum computing. Hereby, the strained quantum well layers are fabricated by the pseudomorphic growth of Si and Ge on SiGe. The strain partially splits the respective band energy degeneracy as a prerequisite for eventual qubit operation. Consequently, the local variations in this strain (e.g., by misfit dislocations) cause local variations in the valley splitting[8,9] and also bring charge noises,[10] which were shown to influence the quantum coherence of qubit states negatively. Hence, on the way to scale up quantum computer to a large number of spin qubits hosted in Si or Ge quantum well layers,[11,12] it is of superior importance for the quality of qubits to achieve decent and homogeneous strain in the quantum well layers. This can only be realized by a deep understanding and ultimately the prevention of the strain

relaxation accompanied by the misfit dislocation formation and propagation in such quantum well layers.

The misfit dislocations in the SiGe-based materials were carefully studied in the last century. Matthews and Blakeslee[13] described the plastic strain relaxation accompanied by the formation and propagation of misfit dislocations when the strained layer exceeds a critical thickness. Later on, Dodson and Tsao[14] stated that the misfit dislocation propagation is a thermally activated process. In their statement, the misfit dislocation propagation velocity is related to both the stress on the epitaxial layer and the temperature it suffers. In addition, Freund[15] studied that the misfit dislocation propagation can also be blocked due to the strain field barrier from other perpendicular misfit dislocations. When the strained layer thickness is above another critical value, the propagation can overcome the barrier and be unblocked. In the case of SiGe heterostructures for qubits, we have investigated[16] the formation of misfit dislocation in the Si quantum well layers, when they

exceed the critical thickness defined by the Matthews–Blakeslee criterion. The layers were grown by chemical vapor deposition (CVD) at relatively high temperatures. Later, we found[17] that the strained Si layer grown by molecular beam epitaxy (MBE) at a lower temperature on the relaxed $Si_{0.7}Ge_{0.3}$ buffer has no misfit dislocation presented even when the Si layer exceeds the critical thickness. These studies suggest that not only the layer thickness influences the formation of misfit dislocation, but the temperature also does.

In this work, we investigate the misfit dislocation propagation in the strained Si layer on $Si_{0.7}Ge_{0.3}$ buffer during post-growth annealing at temperatures from 500 to 600 °C by electron channeling contrast imaging (ECCI) technique. By plotting the dislocation propagation velocities over the inverse temperature, we obtained an Arrhenius-type plot, from which the activation barriers of the propagation are extracted. The same experiment was performed at the strained Ge layer grown by MBE at 270 °C on the relaxed $Si_{0.3}Ge_{0.7}$ buffer. The annealing temperatures were from 300 to 400 °C. The misfit dislocation propagation blocking by other misfit dislocations occurs in 10 nm Si but not in 20 nm Ge, which has a good agreement with the criterion proposed by Freund.[15] In this case, the influence of the blocking interactions on strain relaxation in these layers is further calculated. Our results show that strain relaxation happens not only during the epitaxial growth but also during the post-growth annealing. Based on these observations, we can propose that the misfit dislocation propagation in the Si or Ge quantum well layer for qubits can be suppressed kinetically by reducing the epitaxy temperature and the temperature applied in post-epitaxy device fabrication processes.

II. GENERAL CONCEPTS

The strain relaxation by the misfit dislocation formation is described in detail in our previous work.[16] In this work, we are going to further discuss the misfit dislocation propagation kinetics in strained epitaxial layers, which was studied by Dodson and Tsao, as well as the dislocation blocking interactions studied by Freund.

Below, an important parameter misfit strain ε is defined as the misfit from the substrate to the film:

$$\varepsilon = \frac{a_{\text{substrate}} - a_{\text{film}}}{a_{\text{film}}}, \tag{1}$$

where $a_{\text{substrate}}$ and a_{film} are the in-plane lattice constants of substrates and films under the strain relaxed condition, respectively.

A. Threading dislocation gliding kinetics—Dodson–Tsao law

The strain relaxation due to misfit dislocation propagation by threading dislocation gliding is a thermally activated process.[18] The propagation velocity v can be written with a simple Arrhenius-type law as

$$v = v_0(\sigma) \exp\left(-\frac{E_a(\sigma)}{kT}\right). \tag{2}$$

The pre-exponential factor $v_0(\sigma)$ and the activation energy $E_a(\sigma)$ depend on the material and the stress applied σ. In addition, k is

the Boltzmann constant and T is the temperature applied. The stress-dependence of $E_a(\sigma)$ is given as follows:

$$E_a(\sigma) = E_0\left(1 - \frac{|\sigma|}{\tau_0}\right). \tag{3}$$

Here, E_0 is the propagation activation energy at zero stress. τ_0 is the so-called zero-temperature flow stress, which is roughly 5 %–10 % of the shear modulus in semiconductors,[19] while it is around 1 % in metals. The stress σ here is related to the misfit strain ε in the layer by

$$\sigma = 2\varepsilon\mu\frac{1 + \nu}{1 - \nu}, \tag{4}$$

where μ is the shear modulus and ν is the Poisson ratio.

Hence, according to Eqs. (2) and (3), the propagation velocity increases with the temperature and stress. This stress-dependent misfit dislocation propagation kinetics stated by Dodson and Tsao was also experimentally verified by the relaxation of SiGe films grown by MBE on the Si substrate.[20–22]

B. Dislocation blocking mechanism—Freund criterion

During the misfit dislocation propagation in the strained layer, it can interact with another misfit dislocation at the interface. This interaction will block the propagation because of the strain field associated with the other misfit dislocation [Fig. 1(b)]. When the layer is grown thicker, the force from the misfit strain on the misfit dislocation propagation will increase and can overcome the blocking effect from the other misfit dislocations. That leads to the unblocking of the propagation [Fig. 1(c)].

Freund proposes a simple model[15] to calculate the criterion for the bypass of the misfit dislocation propagation above the other misfit dislocations. The detailed calculation is described in Appendix A.

From the calculation, the critical thickness h_F for the unblocking of the misfit dislocations in the strained Si or Ge layers with regard to their strains ε is plotted in Fig. 2. The critical thickness of the dislocation blocking of the Si with 1.1% strain and Ge with 1.3% strain is underlined because they are the samples investigated in this work. It needs to mention that h_F here is slightly larger from the simplified calculation model without taking the Burgers vectors of the dislocations into consideration.

The blocking and unblocking effects are experimentally observed already in SiGe films on Si.[23,24]

III. EXPERIMENTAL DETAILS

The epitaxial growth of the SiGe heterostructures in this work was carried out by a hybrid MBE/CVD technique.[17] The relaxed $Si_{0.7}Ge_{0.3}$[17] and $Si_{0.3}Ge_{0.7}$[25,26] substrate was grown on (0 0 1) Si wafer by reduced pressure and atmospheric CVD, respectively. Chemical mechanical polishing (CMP) was used to remove the cross-hatch surface roughness of the relaxed buffer layers. The $Si_{0.7}Ge_{0.3}$ substrates have a threading dislocation density of around 1×10^7 cm^{-2}, while the $Si_{0.3}Ge_{0.7}$ substrates have a threading dislocation density of 5×10^5 cm^{-2}. Surface preparations combining wet
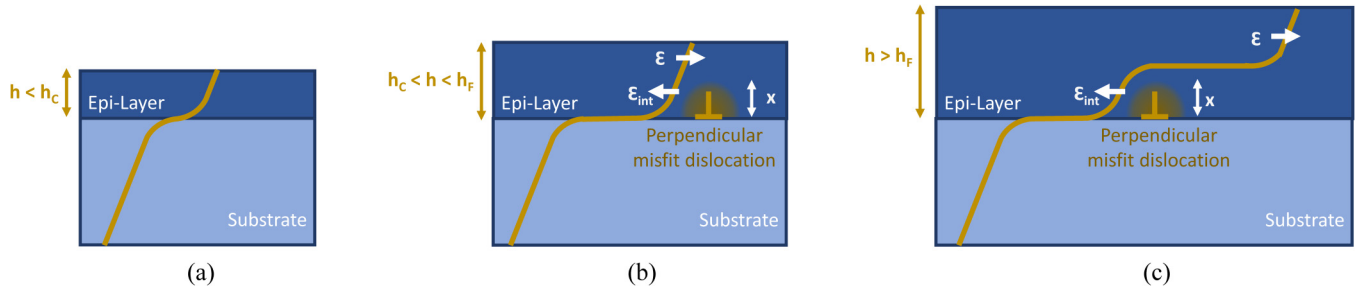
FIG. 1. Schematic diagram showing the blocking mechanism on the misfit dislocation propagation from a perpendicular misfit dislocation when the epitaxial layer exceeds the critical thickness h_c defined by the Matthews–Blakeslee criterion. (a) The propagation is forced by the stress from the misfit strain ε. (b) The misfit dislocation propagation can be blocked by a perpendicular misfit dislocation due to the strain field around it causes. The fact can be described as an effective strain reduction induced by the perpendicular dislocation as ε_{int}. ε_{int} is positively related to the distance from the misfit dislocation x. (c) When the layer is thicker, the effect of the perpendicular misfit dislocation is weaker. When the layer is above h_F defined by the Freund criterion, the threading dislocation can overcome the barrier from the perpendicular misfit dislocation and glide to propagate the misfit dislocation further, that is called unblocking.

chemical cleaning and *in situ* annealing and atom hydrogen irradiation at 700 °C were done on these SiGe substrates. Afterward, 10 nm ^{28}Si/50 nm ^{28}Si$_{0.7}$Ge$_{0.3}$ or 20 nm Ge/30 nm ^{28}Si$_{0.3}$Ge$_{0.7}$ was grown on the top of these relaxed SiGe substrates by an MBE equipped with electron beam evaporators for both ^{28}Si and Ge. The sketches of these epitaxial layers are shown in Figs. 3(a) and 3(f).

The annealing of the strained Si and Ge layers was performed on the pieces from the same wafer in a UHV chamber with a vacuum of around 1×10^{-7} mbar at different temperatures for 10 min. The annealing temperatures were chosen by the ones slightly higher than the growth temperatures (listed in Fig. 3). Before annealing, the heater was preheated for at least 10 min, and the sample was delivered into the annealing position within 1 min. After annealing, the sample was moved out from the annealing position immediately.

To investigate the defects in these layers, the electron channeling contrast imaging (ECCI) was performed in a Thermo Fisher Scientific's Apreo scanning electron microscope at 10 kV and 3.2 nA for the misfit dislocation detection in the layer stacks close to the surfaces.
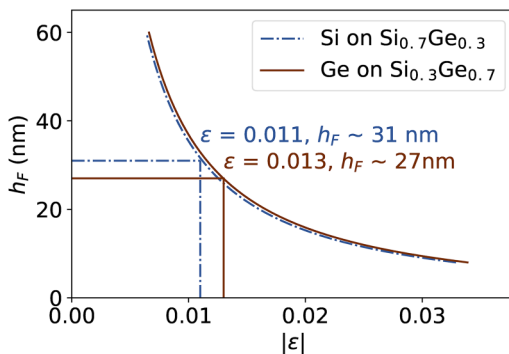

FIG. 2. The critical thickness h_F converted from h/b (Fig. 6 in Appendix A) for the unblocking of the propagation with regard to certain strain ε in the system of the Si or Ge layer on relaxed SiGe substrates.

IV. RESULTS

A. Misfit dislocation propagation under thermal annealing

Figure 3 presents the schematics of the studied strained Si layer as well as the strained Ge layer. The Si layer has 1.1 % tensile strain, and the Ge layer has 1.3 % compressive strain.[27] Figures 3(b) and 3(e) show the ECCI images of the misfit dislocation network in the as-grown and post-growth annealed Si layers. The orthogonal dislocations lie along two $\langle 110 \rangle$ directions at the interface between the strained layers and the relaxed SiGe buffer, and their average length of misfit dislocations develops obviously with the increasing annealing temperatures. Figures 3(g)–3(j), respectively, show the misfit dislocation network in the strained Ge layer. The misfit dislocation networks show similar development with increasing post-growth annealing temperatures.

The misfit dislocation propagation velocities can be measured by dividing the average misfit dislocation lengths by the annealing time, 10 min. The measured velocities are plotted on Arrhenius curves in Fig. 4 in regard to the modified annealing temperatures. The fitted activation energy from Eq. (3) of the threading dislocation gliding is 0.49 ± 0.01 eV in the strained Si and 0.39 ± 0.10 eV in strained Ge, where the errors are from the linear regression fitting. The temperature modification is performed considering the heat radiation exchange between the graphite heater and the emission character from the molybdenum sample holder, which is described in detail in Appendix B.

The theoretical values of the activation energies of the misfit dislocation propagation gliding calculated from the Dodson–Tsao law and their experimental values from Fig. 4 are listed in Table I. The theoretical activation energies have big ranges because τ_0 in Eq. (3) is 5%–10% of the shear modulus in semiconductors. Table I shows the agreement between the theoretical and the experimental activation energies.

It is worth mentioning that there are some characteristic differences between the misfit dislocation networks in the strained Si layers and in the strained Ge layers. In Fig. 3(e), the misfit dislocations often end when they meet other perpendicular misfit
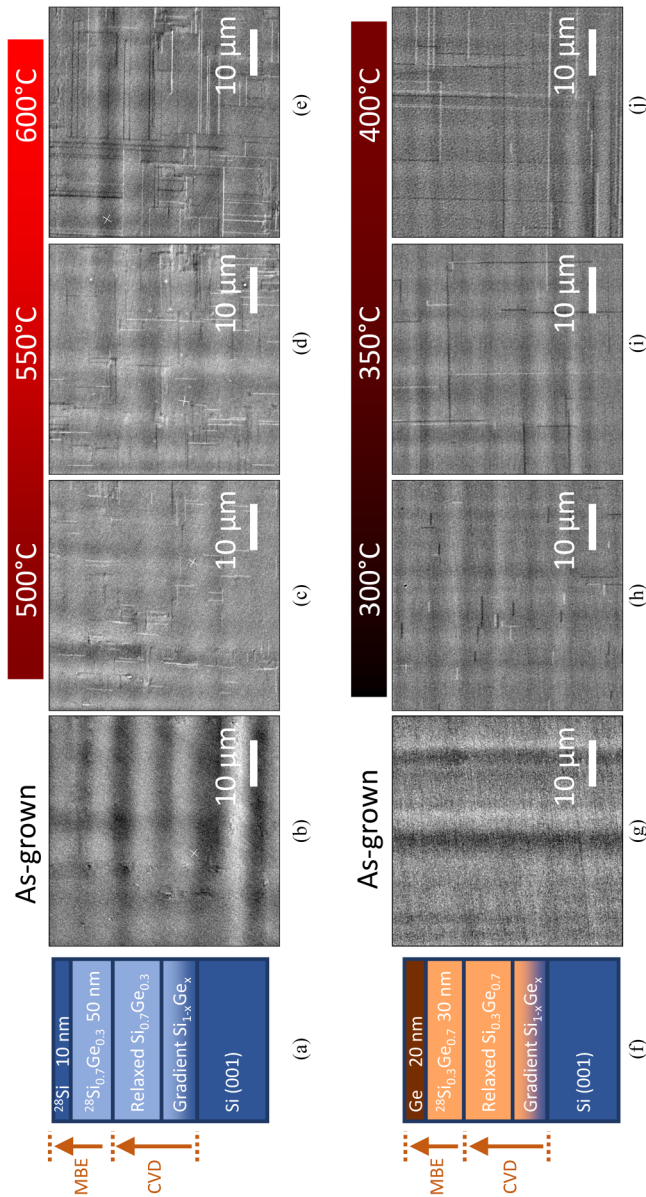
FIG. 3. Schematic cross sections of (a) the strained Si layer on relaxed ^{28}Si$_{0.7}$Ge$_{0.3}$ or (f) the strained Ge layer on relaxed ^{28}Si$_{0.3}$Ge$_{0.7}$ realized by a hybrid MBE/CVD technique. ECCI images showing dislocation in the strained Si and Ge layers: (b) the as-grown Si layer presents no misfit dislocation; the misfit dislocations form in the Si layer through the annealing at temperatures from 500 to 600 °C [(c)–(e)] for 10 min; similarly, the as-grown Ge layer presents no misfit dislocation (g); the misfit dislocations form in the Ge layer through annealing at temperatures from 300 to 400 °C [(h)–(j)] for 10 min. The annealing temperatures are indicated above the ECCI images.

dislocations. That is not the case in Fig. 3(j), where the perpendicular misfit dislocations cross over each other. This feature of the misfit dislocation network in Si matches well with the blocking mechanism between the perpendicular misfit dislocations, which

was also observed in our previous study on the strained Si layer grown by CVD:[16] the misfit dislocation propagation is blocked by perpendicular misfit dislocations. The reason why the misfit dislocations in the strained Ge layer overcome this blocking mechanism is that the Ge layer is thicker than the Si layer. The thickness of the Ge layer as 20 nm is approaching the critical value for unblocking mechanism (Fig. 2). Since both the Si$_{0.7}$Ge$_{0.3}$ and Si$_{0.3}$Ge$_{0.7}$ substrates are flattened by CMP, the blocking effect from surface roughness on misfit dislocations is out of consideration here.

These blocking and unblocking mechanisms from the dislocation interactions can also influence the experimental propagation velocity measurement and further the derived activation energies in Table I. When the blocking interaction happens, the experimental dislocation average lengths tend to be shorter since the dislocation propagation stops earlier.[20,28] This can explain that the experimental activation energy in the strained Si layer lies on the lower end of the theoretical range, respectively, that it lies in the middle of the theoretical activation energy range in the case of the strained Ge layer in Table I.

B. Strain relaxation with misfit dislocation network

The experimental results above show that the misfit dislocations form by threading dislocation bending and propagate in the strained Si and Ge layers due to post-growth annealing. However, the blocking interactions between misfit dislocation only happen in the strained Ge layers because of their larger thickness. Here, we will further calculate the dependence of the relaxation in the epitaxial layer on the threading dislocation density and also the misfit dislocation blocking interactions.

During the calculation, the geometry of the sample is taken as a square of 1×1 mm^2 with edges along $\langle 1\,1\,0 \rangle$. This is taken approximately by the sample piece of the annealing experiments above.

The strain relaxation $\varepsilon_{\text{relax}}$ by misfit dislocations in epitaxial layers can be described as[13]

$$|\varepsilon_{\text{relax}}| = \frac{|\mathbf{b}|}{\gamma d_{\text{MD}}}, \tag{5}$$

where **b** is the Burgers vector of the dislocations and d_{MD} is the misfit dislocation spacing. γ depends on the relaxation efficiency of the misfit dislocations, that is related to the dislocation type. For the 60° misfit dislocations in diamond-type semiconductors, $\gamma = 2$.[29] It reveals that the strain in the layer gets more relaxed with denser misfit dislocations.

The misfit dislocation spacing can be calculated from the misfit dislocation network,[16] from the length sum of misfit dislocations A in a certain area $\sum l_i$ by

$$d_{\text{MD}} = \frac{A}{\sum l_i}. \tag{6}$$

From the misfit dislocation formation mechanism by Matthews and Blakeslee and also our previous observation in Ref. 16, every pre-existing threading dislocation is a source of a misfit dislocation. Therefore, the misfit dislocation network in the strained layer is related to the threading dislocation spacing d_{TD}, which is related to
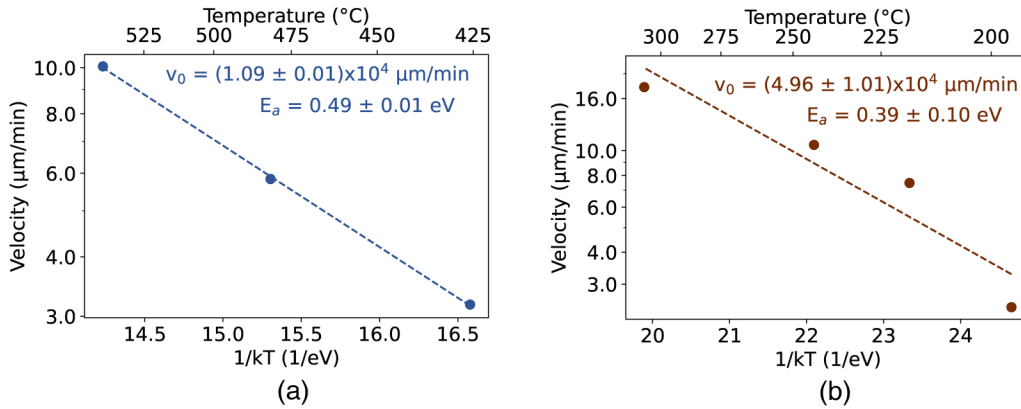
09 August 2023 07:01:02

FIG. 4. The Arrhenius-type plots of the misfit dislocation propagation in the strained Si layer (a) and in the strained Ge layer (b). The measurements are fitted into Eq. (2), where v_0 and E_a from fitting are listed in the figures. The temperatures here are corrected according to Appendix B.

the threading dislocation density TDD,

$$d_{\text{TD}} = \frac{1}{\sqrt{\text{TDD}}}. \tag{7}$$

To conduct further calculation of the effect of the threading dislocation density and the blocking interactions on the strain relaxation, two different conditions are considered here:

(1) The first condition is that the blocking interaction between misfit dislocations happens. According to a Monte Carlo simulation of the strain relaxation of Si on SiGe from our group,[29] the threading dislocation spacing d_{TD} and the misfit dislocation spacing d_{MD} have a roughly constant ratio of around 2 and are independent of the sample size. Merging Eqs. (5) and (7), and the constant ratio $\frac{d_{\text{TD}}}{d_{\text{MD}}} = 2$ together, the correlation of relaxation and threading dislocation density TDD can be written as

$$\varepsilon_{\text{relax}} = \frac{|\mathbf{b}|}{\gamma d_{\text{MD}}} = \frac{|\mathbf{b}|}{2 \cdot \frac{1}{2} d_{\text{TD}}} = \frac{|\mathbf{b}|}{2 \cdot \frac{1}{2} \sqrt{\frac{1}{\text{TDD}}}} = |\mathbf{b}| \sqrt{\text{TDD}}. \tag{8}$$

(2) The second condition is that the blocking interaction between misfit dislocations does not happen. The misfit dislocation can extend till the end of the wafer. In this case, the average misfit dislocation length is assumed as the half size of the wafer in the square geometry applied. With the sample length $a = 1$ mm, the average length of misfit dislocation is reasonably assumed as $\frac{a}{2}$. The

number of misfit dislocations equals the number of threading dislocations x, which means

$$x = \text{TDD} \cdot a^2. \tag{9}$$

According to Eq. (6), misfit dislocation spacing d_{MD} is

$$d_{\text{MD}} = \frac{a^2}{x \cdot \frac{a}{2}} = \frac{2a}{x}. \tag{10}$$

Introducing Eqs. (9) and (10) into Eq. (5), the relaxation when the misfit dislocations do not block each other is

$$\varepsilon_{\text{relax}} = \frac{|\mathbf{b}|}{\gamma d_{\text{MD}}} = \frac{|\mathbf{b}| \cdot a \cdot \text{TDD}}{4}. \tag{11}$$

The correlations between relaxation and threading dislocation density TDD in both conditions with [Eq. (8)] or without [Eq. (11)] blocking interaction between misfit dislocations are plotted in Fig. 5. The misfit strain levels of the unrelaxed Si on $\text{Si}_{0.7}\text{Ge}_{0.3}$ and Ge on $\text{Si}_{0.3}\text{Ge}_{0.7}$ are also indicated in Fig. 5. From here, the relaxation with the blocking effect is significantly less than without blocking. In addition, the increase in strain relaxation with regard to TDD is also severe without the blocking interactions. The relaxation levels of the strained Si in Fig. 3(e) and the strained Ge in Fig. 3(j) based on their misfit dislocation spacing d_{MD} are

TABLE I. The experimental and theoretical activation energies of the misfit dislocation propagation.

Material system	Strain	E_a (Experimental)	E_a (Theoretical)
10 nm strained Si on relaxed $\text{Si}_{0.7}\text{Ge}_{0.3}$	1.1 % tensile	0.49 ± 0.01 eV	0.44 – 1.32 eV[a]
20 nm strained Ge on relaxed $\text{Si}_{0.3}\text{Ge}_{0.7}$	1.3 % compressive	0.39 ± 0.10 eV	0.14 – 0.87 eV[a]

[a]The variant energies are calculated based on the zero-temperature flow stress τ_0 in Eq. (3), which is roughly 5 %–10 % of the shear modulus in semiconductors.[19]
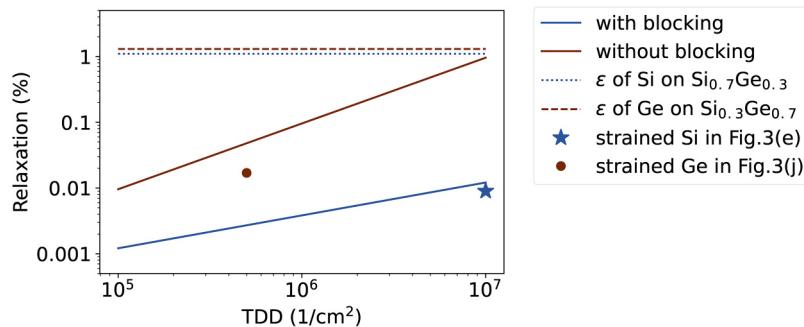
FIG. 5. The dependence of the strain relaxation in the Si or Ge layers on the threading dislocation density in two conditions: the blocking interaction happens between the misfit dislocations (blue line); the blocking interaction does not happen between misfit dislocations (brown line). The misfit strains of the Si layer on $Si_{0.7}Ge_{0.3}$ the Ge layer on $Si_{0.3}Ge_{0.7}$ and are 1.1 % and 1.3 % marked as dotted and dashed lines here. The analyzed relaxation levels of layers in Figs. 3(e) and 3(j) are noted as well.

marked in Fig. 5. The strained relaxation in Si fits well with the calculation. However, the strain relaxation in Ge is lower than calculation.

Here, only square geometry with a small sample piece as $1 \times 1 \, mm^2$ is applied. With other geometry, the correlation between strain relaxation and TDD is slightly different as it is shown in Fig. 5.

V. DISCUSSIONS AND CONCLUSIONS

Combining the results from this work, we arrive at several thoughts regarding the misfit dislocations in SiGe heterostructures for qubits,

(1) When the Si or Ge quantum well layers in SiGe heterostructures for qubits are often above the critical thickness of misfit dislocation formation defined by the Matthew–Blakeslee criterion, the epitaxial growth of the heterostructures by MBE performed at low temperatures can suppress the misfit dislocation formation kinetically compared to CVD, which generally utilizes higher growth temperature.

(2) Although the growth can happen at a lower temperature in MBE, the post-growth processes like the oxide layer deposition often happen at 300 °C;[5,30] the ohmic contact for the Ge layer often happens at around 400 °C[31] and, for the Si layer, happens at 700 °C.[1] These post-growth processes can potentially activate the misfit dislocation propagation. Noticeably, according to Refs. 32 and 33, the misfit dislocation propagation in a buried strained Si or Ge layer in the SiGe heterostructure is probably slightly slower than the propagation in an unburied strained layer. This is because the misfit dislocation propagation in the buried layer needs to form double kinks compared to the single-kink dominated propagation in an unburied layer.

(3) According to our findings, a thermal budget for the post-growth processes can be reasonably suggested as $0.5 \, T_m$ according to the study of Dodson and Tsao.[14,34] If the post-growth annealing must access this thermal budget, shortening the annealing time is also a way to suppress the misfit dislocation propagation kinetically.

In summary, the misfit dislocation kinetics and interaction are studied in this work. The MBE as-grown strained Si layer on relaxed $Si_{0.7}Ge_{0.3}$ and the strained Ge layer on relaxed $Si_{0.3}Ge_{0.7}$ are free of misfit dislocations even though their thicknesses are above

the critical thickness. Misfit dislocations form at the interface of the strained layers due to the gliding of the pre-existing threading dislocations during post-growth annealing. The misfit dislocation propagation velocity increases with the annealing temperatures exponentially. The activation energies of the propagation are derived from the Arrhenius-type equation, and they agree well with the stress-dependent dislocation kinetics stated by Dodson and Tsao.[18] Furthermore, the misfit dislocation propagation in the strained Si layer is blocked by the perpendicular misfit dislocations, where the propagation in the strained Ge layer is unblocked. These facts are due to the thickness difference between the stained Si and the strained Ge layers. The strained Si layer here is quite thin so that the misfit dislocation propagation cannot overcome the strain barrier from the other perpendicular misfit dislocation. It is the other case in the strained Ge layer here. In addition, we also calculate that the misfit dislocation networks are supposed to be significantly denser without the blocking effect when the substrate has the same threading dislocation densities.

Together, we believe that this work enables the understanding of the strain relaxation process with misfit dislocation formation and propagation in the SiGe heterostructures for both electron spin qubits and hole spin qubits.

AUTHOR DECLARATIONS
Conflict of Interest

The authors have no conflicts to disclose.

09 August 2023 07:01:02

Author Contributions

Yujia Liu: Conceptualization (equal); Data curation (equal); Formal analysis (equal); Resources (equal); Validation (equal); Visualization (equal); Writing – original draft (equal). **Kevin-Peter Gradwohl:** Conceptualization (equal); Resources (equal); Supervision (equal); Writing – review & editing (equal). **Chen-Hsun Lu:** Investigation (lead); Methodology (lead); Writing – review & editing (equal). **Kaspars Dadzis:** Data curation (equal); Investigation (equal); Validation (equal); Writing – review & editing (equal). **Yuji Yamamoto:** Resources (equal). **Lucas Becker:** Resources (equal). **Peter Storck:** Resources (equal). **Thilo Remmele:** Investigation (equal); Methodology (equal). **Torsten Boeck:** Funding acquisition (lead); Project administration (lead); Supervision (equal). **Carsten Richter:** Conceptualization (equal); Funding acquisition (lead); Project administration (lead); Supervision (equal); Writing – review & editing (equal). **Martin Albrecht:** Conceptualization (lead); Funding acquisition (equal); Methodology (lead); Project administration (equal); Supervision (equal).

DATA AVAILABILITY

The data that support the findings of this study are available from the corresponding author upon reasonable request.

APPENDIX A: SIMPLIFIED MODEL OF FREUND CRITERION FOR MISFIT DISLOCATION BLOCKING

Here, we will briefly introduce a simplified model from Freund[15] to calculate the criterion of misfit dislocation blocking interaction.

As it is shown in Fig. 1, the strain originated from the other misfit dislocation to compensate the misfit strain ε at the distance x from the heterointerface is

$$|\varepsilon_{\text{int}}| = \frac{1}{2\pi}\frac{|\mathbf{b}|}{x}, \tag{A1}$$

where $\mathbf{b}$ is the Burgers vector of the dislocation. Therefore, the effective strain ε_{eff} at the distance x from the heterointerface is

$$\varepsilon_{\text{eff}} = \varepsilon - \varepsilon_{\text{int}}, \tag{A2}$$

where ε is the misfit strain. The remaining distance to the surface is denoted by

$$h_* = h - x. \tag{A3}$$

The propagation is unblocked, when the effective strain fits the rudimentary critical condition for the threading dislocation above x to glide. This simplified critical condition from Freund can be written as

$$|\varepsilon_{\text{eff}}| = \frac{|\mathbf{b}|}{4\pi h_*}\ln\frac{8h_*}{|\mathbf{b}|}, \tag{A4}$$

where the dislocation cutoff radius as $\frac{|\mathbf{b}|}{4}$ is considered and poison ratio $v = 0.3$ in Si, a Ge related material system is applied.

Combining Eq. (A1), (A2), and (A4), it gives

$$|\varepsilon| = \frac{1}{2\pi}\frac{|\mathbf{b}|}{x} + \frac{|\mathbf{b}|}{4\pi h_*}\ln\frac{8h_*}{|\mathbf{b}|}. \tag{A5}$$

The condition to get the minimal ε respective to h_* is that

$$\frac{d|\varepsilon|}{dh_*} = 0. \tag{A6}$$

By solving h_* and substituting h_* into Eq. (A5), the minimal misfit strain ε with regard to the strained Si or Ge layer thickness for the unblocking mechanism is plotted in Figs. 2 and 6.

Noticeably, the blocking criterion depends also on the Burgers vectors of the misfit dislocations. Freund states that the critical thickness of the blocking in this simple model is expected slightly higher.

APPENDIX B: ANNEALING TEMPERATURE MODIFICATION

According to the Dodson–Tsao law [Eq. (2)], the activation energies E_a can be obtained from the functional dependency of the misfit dislocation propagation velocity on the annealing temperature. The annealing experiments were done by putting the samples on a molybdenum holder under a pre-heated heater and taking the sample with the holder out of the heating immediately after annealing for 10 min. Since the samples take time for heat-up and cool-down, just taking the dislocation propagation velocities calculated with 10 min and the respective preset annealing temperatures into Eq. (2) would lead to a systematic error in the activation energy. Hence, it is necessary to determine the temperature history of the samples as a function of time, which is done here. Then, annealing temperatures can be modified and then applied to the Eq. (2).

We applied the temperature modification with the molybdenum holder because the molybdenum holder is ten times bigger than the samples. This means in the text, T, means both the temperature of the molybdenum holder and the sample.

Generally, the misfit dislocation length L can be obtained by integrating Eq. (2),

$$L = \int_{t_0}^{t} v_0 \exp\left(\frac{-E_a}{kT(t)}\right)dt, \tag{B1}$$

where t is the time and $T(t)$ is the temperature of the sample (also the sample holder) with respect to time including the heating up and cooling down. When $T(t)$ is substituted with a fixed modified temperature T^* and t is substituted with a fixed time $t^* = 10$ min, it can be rewritten as

$$L = v_0\exp\left(\frac{-E_a}{kT^*}\right)t^*. \tag{B2}$$

Now, T^* can be determined combining Eqs. (B1) and (B2). The remaining question here is the temperature history $T(t)$.

Several conditions are assumed to solve $T(t)$: In the calculation, only the heat radiation is considered. The heat convection by gas motion is ignored because the annealing happens in ultra high vacuum. The heat conduction is ignored because only a small part
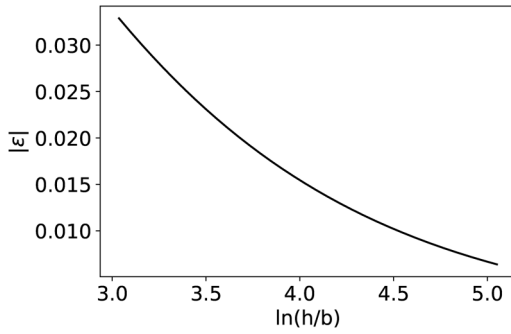
09 August 2023 07:01:02

FIG. 6. The minimal misfit strain ε forcing the misfit dislocation propagation to bypass the barrier of the perpendicular misfit dislocation in the epitaxial layer with certain thickness h/b, calculated from Eq. (A5).

of the substrate holder is touched with the supporting ring. The radiation of the MBE chamber is ignored because it is cold. In addition, a one-dimensional model is applied here since the annealing happens in the middle of the substrate holder and the temperature is likely homogeneous horizontally.

The heat power $P(T)$ the molybdenum holder obtained is equal to the heat radiation from the heater P_{heater} minus the emitted heat on two sides of the holder P_{holder}. Since the surface area of the holder and the heater are the same,

$$P(T) = P_{\text{heater}} - P_{\text{holder}}, \qquad (B3)$$

$$= \varepsilon_{\text{heater}} \, \sigma \, T_{\text{heater}}^{\,4} - 2\varepsilon_{\text{Mo}} \, \sigma \, T^4, \qquad (B4)$$

where ε is emissivity and σ is the Stefan–Boltzmann constant. Here, $\varepsilon_{\text{heater}} = 1$ and $\varepsilon_{\text{Mo}} = 0.2$ for molybdenum holder.[35]

Since the heater is switched on in advance and its temperature is held constant by a power control in the experiment, it is assumed
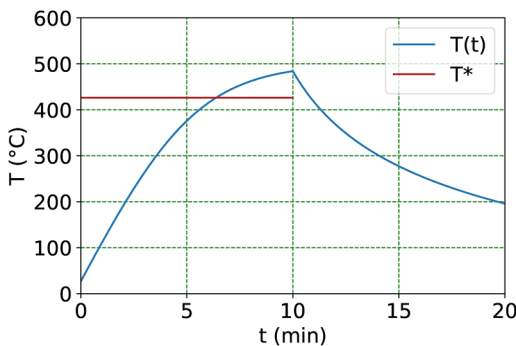

FIG. 7. Simulation of molybdenum holder temperature T during the heat-up and cool-down processes at the set temperature $T_{\text{set}} = 500\,°\text{C}$. The modified temperature T^* over $t^* = 10\,\text{min}$ is also sketched. The modification is based on the integration of the misfit dislocation propagation during the 10 min heat-up and the 10 min cool-down.

that the temperature of the heater stays the same when the holder is added. When the holder temperature T reaches the target set temperatures, the system is in equilibrium. So,

$$P(T_{\text{set}}) = \varepsilon_{\text{heater}} \, \sigma \, T_{\text{heater}}^{\,4} - 2\varepsilon_{\text{Mo}} \, \sigma \, T_{\text{set}}^{\,4} = 0, \qquad (B5)$$

which tells the heater temperature T_{heater} by each set temperature T_{set}.

During the heat-up and cool-down processes, the heat absorbed by the holder results in the temperature increase of the holder,

$$CdT = P(T)dt, \qquad (B6)$$

where C is the heat capacity of the molybdenum holder and can be calculated with the holder thickness ($2\,\text{mm}$), the specific heat ($0.25\,\text{J}\,\text{g}^{-1}\,\text{K}^{-1}$), and the density ($10.2\,\text{g}\,\text{cm}^{-3}$) from molybdenum.

We substitute $P(T)$ from Eq. (B4) into Eq. (B6) and do the integration, and then, we get

$$CdT = (\varepsilon_{\text{heater}} \, \sigma T_{\text{heater}}^{\,4} - 2\varepsilon_{\text{Mo}} \, \sigma T^4)dt, \qquad (B7)$$

$$\int_{T_0}^{T} \frac{C}{\varepsilon_{\text{heater}} \, \sigma T_{\text{heater}}^{\,4} - 2\varepsilon_{\text{Mo}} \, \sigma T^4} \, dT = \int_{t_0}^{t} dt. \qquad (B8)$$

By numerically solving the ordinary differential equation (B8), we can get the temperature T over the time t.

For cooling down when the sample with molybdenum holder is taken away from the holder,

$$P_{\text{heater}} = 0. \qquad (B9)$$

Now, Eq. (B4) is rewritten as

$$P(T) = 0 - 2\varepsilon_{\text{Mo}}\sigma T^4. \qquad (B10)$$

When substituting $P(T)$ from Eq. (B10) into Eq. (B6) and do the integration, we can get the temperature T over time t during cooling down.

Taking the experimental annealing time as 10 min and also cooling, the temperature versus time is plotted in Fig. 7. The cooling time is chosen for 10 min with the reason that the misfit dislocation propagation velocity decreases with temperature exponentially; thus, a lower temperature range is not essential. With $T(t)$, the misfit dislocation length L and the modified temperature T^* can be calculated with Eqs. (B2) and (B8), subsequently with respect to each preset temperature T_{set}.

REFERENCES

[1]E. Kawakami, P. Scarlino, D. R. Ward, F. R. Braakman, D. E. Savage, M. G. Lagally, M. Friesen, S. N. Coppersmith, M. A. Eriksson, and L. M. Vandersypen, "Electrical control of a long-lived spin qubit in a Si/SiGe quantum dot," Nat. Nanotechnol. **9**, 666–670 (2014).

[2]X. Mi, M. Benito, S. Putz, D. M. Zajac, J. M. Taylor, G. Burkard, and J. R. Petta, "A coherent spin-photon interface in silicon," Nature **555**, 599–603 (2018).

[3]T. Struck, A. Hollmann, F. Schauer, O. Fedorets, A. Schmidbauer, K. Sawano, H. Riemann, N. V. Abrosimov, Ł. Cywiński, D. Bougeard, and L. R. Schreiber,

09 August 2023 07:01:02

"Low-frequency spin qubit energy splitting noise in highly purified 28Si/SiGe," npj Quantum Inf. **6**, 40 (2020).

[4]A. Hollmann, T. Struck, V. Langrock, A. Schmidbauer, F. Schauer, T. Leonhardt, K. Sawano, H. Riemann, N. V. Abrosimov, D. Bougeard, and L. R. Schreiber, "Large, tunable valley splitting and single-spin relaxation mechanisms in a Si/Si$_x$Ge$_{1-x}$ quantum dot," Phys. Rev. Appl. **13**, 1 (2020).

[5]N. W. Hendrickx, W. I. Lawrie, L. Petit, A. Sammak, G. Scappucci, and M. Veldhorst, "A single-hole spin qubit," Nat. Commun. **11**, 3478 (2020).

[6]N. W. Hendrickx, D. P. Franke, A. Sammak, G. Scappucci, and M. Veldhorst, "Fast two-qubit logic with holes in germanium," Nature **577**, 487–491 (2020).

[7]N. W. Hendrickx, W. I. Lawrie, M. Russ, F. van Riggelen, S. L. de Snoo, R. N. Schouten, A. Sammak, G. Scappucci, and M. Veldhorst, "A four-qubit germanium quantum processor," Nature **591**, 580–585 (2021).

[8]M. Friesen, S. Chutia, C. Tahan, and S. N. Coppersmith, "Valley splitting theory of SiGe/Si/SiGe quantum wells," Phys. Rev. B **75**, 115318 (2007).

[9]S. Goswami, K. A. Slinker, M. Friesen, L. M. McGuire, J. L. Truitt, C. Tahan, L. J. Klein, J. O. Chu, P. M. Mooney, D. W. Van Der Weide, R. Joynt, S. N. Coppersmith, and M. A. Eriksson, "Controllable valley splitting in silicon quantum devices," Nat. Phys. **3**, 41–45 (2007).

[10]B. P. Wuetz, D. D. Esposti, A. M. J. Zwerver, S. V. Amitonov, M. Botifoll, J. Arbiol, A. Sammak, L. M. K. Vandersypen, M. Russ, and G. Scappucci, "Reducing charge noise in quantum dots by using thin silicon quantum wells," arXiv:2209.07242 (2022).

[11]R. Li, L. Petit, D. P. Franke, J. P. Dehollain, J. Helsen, M. Steudtner, N. K. Thomas, Z. R. Yoscovits, K. J. Singh, S. Wehner, L. M. Vandersypen, J. S. Clarke, and M. Veldhorst, "A crossbar network for silicon quantum dot qubits," Sci. Adv. **4**, eaar3960 (2018).

[12]J. M. Boter, J. P. Dehollain, J. P. Van Dijk, Y. Xu, T. Hensgens, R. Versluis, H. W. Naus, J. S. Clarke, M. Veldhorst, F. Sebastiano, and L. M. Vandersypen, "Spiderweb array: A sparse spin-qubit array," Phys. Rev. Appl. **18**, 024053 (2022).

[13]J. W. Matthews and A. E. Blakeslee, "Defects in epitaxial multilayers: I. Misfit dislocations," J. Cryst. Growth **27**, 118–125 (1974).

[14]B. W. Dodson and J. Y. Tsao, "Non-Newtonian strain relaxation in highly strained SiGe heterostructures," Appl. Phys. Lett. **53**, 2498–2500 (1988).

[15]L. B. Freund, "A criterion for arrest of a threading dislocation in a strained epitaxial layer due to an interface misfit dislocation in its path," J. Appl. Phys. **68**, 2073–2080 (1990).

[16]Y. Liu, K.-P. Gradwohl, C.-H. Lu, T. Remmele, Y. Yamamoto, M. H. Zoellner, T. Schroeder, T. Boeck, H. Amari, C. Richter, and M. Albrecht, "Role of critical thickness in SiGe/Si/SiGe heterostructure design for qubits," J. Appl. Phys. **132**, 085302 (2022).

[17]Y. Liu, K.-P. Gradwohl, C.-H. Lu, Y. Yamamoto, T. Remmele, C. Corley-Wiciak, T. Teubner, C. Richter, M. Albrecht, and T. Boeck, "Growth of 28Si quantum well layers for qubits by a hybrid MBE/CVD technique," ECS J. Solid State Sci. Tech. **12**(2), 024006 (2023).

[18]B. W. Dodson and J. Y. Tsao, "Stress dependence of dislocation glide activation energy in single-crystal silicon-germanium alloys up to 2.6 GPa," Phys. Rev. B **38**, 12383–12387 (1988).

[19]B. W. Dodson and J. Y. Tsao, "Scaling relations for strained-layer relaxation," Appl. Phys. Lett. **55**, 1345–1347 (1989).

[20]R. Hull, J. C. Bean, D. J. Werder, and R. E. Leibenguth, "Activation barriers to strain relaxation in lattice-mismatched epitaxy," Phys. Rev. B **40**, 1681–1684 (1989).

[21]C. G. Tuppen and C. J. Gibbings, "Misfit dislocations in annealed Si$_{1-x}$Ge$_x$/Si heterostructures," Thin Solid Films **183**, 133–139 (1989).

[22]P. Y. Timbrell, J. M. Baribeau, D. J. Lockwood, and J. P. McCaffrey, "An annealing study of strain relaxation and dislocation generation in Si$_{1-x}$Ge$_x$/Si heteroepitaxy," J. Appl. Phys. **67**, 6292–6300 (1990).

[23]E. A. Stach, R. Hull, R. M. Tromp, F. M. Rossi, M. C. Reuter, and J. C. Bean, "*In-situ* transmission electron microscopy studies of the interaction between dislocations in strained SiGe/Si (001) heterostructures," Philos. Mag. A **80**, 1559–2200 (2000).

[24]L. Becker, P. Storck, T. Schulz, M. H. Zoellner, L. D. Gaspere, F. Rovaris, A. Marzegalli, F. Montalenti, M. D. Seta, G. Capellini, G. Schwalb, T. Schroeder, and M. Albrecht, "Controlling the relaxation mechanism of low strain SiGe/Si (001) layers and reducing the threading dislocation density by providing a preexisting dislocation source," J. Appl. Phys. **128**, 215305 (2020).

[25]G. Kozlowski, T. Schroeder, and P. Storck, "Epitaxial growth of low defect SiGe buffer layers for integration of new materials on 300 mm silicon wafers," 2012 Meet. Abstr. **MA2012-02**, 3179 (2012).

[26]M. H. Zoellner, M. I. Richard, G. A. Chahine, P. Zaumseil, C. Reich, G. Capellini, F. Montalenti, A. Marzegalli, Y. H. Xie, T. U. Schülli, M. Häberlen, P. Storck, and T. Schroeder, "Imaging structure and composition homogeneity of 300 mm SiGe virtual substrates for advanced CMOS applications by scanning x-ray diffraction microscopy," ACS Appl. Mater. Interfaces **7**, 9031–9037 (2015).

[27]J. P. Dismukes, L. Ekstrom, E. F. Steigmeier, I. Kudman, and D. S. Beers, "Thermal and electrical properties of heavily doped Ge-Si alloys up to 1300 K," J. Appl. Phys. **35**, 2899–2907 (1964).

[28]V. T. Gillard, W. D. Nix, and L. B. Freund, "Role of dislocation blocking in limiting strain relaxation in heteroepitaxial films," J. Appl. Phys. **76**, 7280–7287 (1994).

[29]K. P. Gradwohl, C. H. Lu, Y. Liu, C. Richter, T. Boeck, J. Martin, and M. Albrecht, "Strain relaxation of Si/SiGe heterostructures by a geometric Monte Carlo approach," Phys. Status Solidi RRL **17**, 2200398 (2022).

[30]P. Boryło, K. Lukaszkowicz, M. Szindler, J. Kubacki, K. Balin, M. Basiaga, and J. Szewczenko, "Structure and properties of Al$_2$O$_3$ thin films deposited by ALD process," Vacuum **131**, 319–326 (2016).

[31]C. Morrison, J. Foronda, P. Wiśniewski, S. D. Rhead, D. R. Leadley, and M. Myronov, "Evidence of strong spin-orbit interaction in strained epitaxial germanium," Thin Solid Films **602**, 84–89 (2016).

[32]R. Hull and J. C. Bean, "In situ observations of misfit dislocations in lattice-mismatched epitaxial semiconductor heterostructures," MRS Bull. **19**, 32–37 (1994).

[33]C. G. Tuppen and C. J. Gibbings, "A quantitative analysis of strain relaxation by misfit dislocation glide in Si$_{1-x}$Ge$_x$/Si heterostructures," J. Appl. Phys. **68**, 1526–1534 (1990).

[34]B. W. Dodson and J. Y. Tsao, "Structural relaxation in metastable strained-layer semiconductors," Annu. Rev. Mater. Sci. **19**, 419–437 (1989).

[35]E. A. Brandes and G. B. Brook, *Smithells Metals Reference Book*, 7th ed. (Reed Educational and Professional Publishing, 1992), pp. 17–26.

09 August 2023 07:01:02